

Article

Wind Shear Model Considering Atmospheric Stability to Improve Accuracy of Wind Resource Assessment

Hongpeng Liu ¹, Guanjin Chen ¹, Zejia Hua ^{1,*}, Jingang Zhang ² and Qing Wang ¹

¹ Engineering Research Centre of Oil Shale Comprehensive Utilization, Ministry of Education, School of Energy and Power Engineering, Northeast Electric Power University, Jilin 132012, China; hongpeng5460@126.com (H.L.); guanjin0212@163.com (G.C.); rlx888@126.com (Q.W.)

² Suzhou THVOW Technology Co., Ltd., Suzhou 215600, China; zhangjingang@126.com

* Correspondence: zejiahua@126.com; Tel.: +86-18686591618

Abstract: An accurate wind shear model is an important prerequisite in extrapolating the wind resource from lower heights to the increasing hub height of wind turbines. Based on the 1-year dataset (collected in 2014) consisting of 15-minute intervals collected at heights of 2, 10, 50, 100, and 150 m on an anemometer tower in northern China, the present study focuses on the time-varying relationship between the wind shear coefficient (WSC) and atmospheric stability and proposes a wind shear model considering atmospheric stability. Through the relationship between Monin–Obukhov (M–O) length and gradient Richardson number, the M–O length is directly calculated by wind data, and the WSC is calculated by combining the Panofsky and Dutton (PD) models, which enhances the engineering practicability of the model. Then, the performance of the model is quantified and compared with two alternative methods: the use of annual average WSC and the use of stability change WSC extrapolation. The analysis demonstrates that the proposed model outperforms the other approaches in terms of normal root mean square error (NRMSE) and normal bias (NB). More specifically, this method reduces the NRMSE and NB by 24–29% and 76–95%, respectively. Meanwhile, it reaches the highest extrapolation accuracy under unstable and stable atmospheric conditions. The results are verified using the Weibull distribution.

Keywords: wind resource assessment; wind shear coefficient; atmospheric stability; wind speed extrapolation



Citation: Liu, H.; Chen, G.; Hua, Z.; Zhang, J.; Wang, Q. Wind Shear Model Considering Atmospheric Stability to Improve Accuracy of Wind Resource Assessment. *Processes* **2024**, *12*, 954. <https://doi.org/10.3390/pr12050954>

Academic Editors: Djamel Hissein Didane and Bukhari Bin Manshoor

Received: 10 April 2024

Revised: 2 May 2024

Accepted: 3 May 2024

Published: 8 May 2024



Copyright: © 2024 by the authors. Licensee MDPI, Basel, Switzerland. This article is an open access article distributed under the terms and conditions of the Creative Commons Attribution (CC BY) license (<https://creativecommons.org/licenses/by/4.0/>).

1. Introduction

The adverse effects of fossil fuels on the environment have led to the adoption of alternative clean and renewable sources of energy such as wind, solar, wave, and hydrogen. Compared with other sources of renewable energy (RE), the installation capacity of wind turbines has increased significantly in recent years [1]. As of 2021, RE contributed to around 29% of the global electricity generation [2]. It is projected that the worldwide installation capacity for wind energy will continue to grow at a faster rate over the next few decades [3,4]. Accordingly, precise wind resource assessment is of significant importance for locating sites, distributing wind turbines, and selecting wind turbine types for new wind farms, as well as enhancing the overall revenue from the existing wind farms. Evaluating the wind energy resource at hub height is one of the main challenges in wind resource assessment [5]. It should be indicated that evaluating wind energy at hub height is an enormous challenge due to limited direct observations and the model simulation resolution [6]. A feasible solution for this problem is to extrapolate the wind power from a lower height to the height of the wind turbine [7].

Among various extrapolation models, the power law (PL) model exhibits reasonable performance [8,9] while having simple mathematical complexity [10], so it is the most widely used model for wind energy purposes [11]. A key parameter of the PL model is

the wind shear coefficient α , which is affected by atmospheric stability [12]. Typically, this parameter is set to $\alpha = 1/7$ [13]. However, studies demonstrate that this assumption leads to reasonable results only under near-neutral atmospheric conditions [14]. Variations in the wind shear coefficient are usually considered as a small disturbance, which is often ignored in calculations [15]. In this context, Wan et al. [14] analyzed various scenarios and demonstrated that the wind shear coefficient is an affecting parameter in the assessment of wind turbine power generation. Furthermore, Gualtieri [12] and Jiale [15] analyzed the influence of atmospheric stability on the wind shear coefficient. The findings revealed that the Panofsky and Dutton (PD) model [16] is the most accurate scheme to determine the wind shear coefficient. However, this model requires various input data, including friction temperature, friction velocity, and the von Karman coefficient for calculating the M-O length (L) [17]. These data are often not included in the wind measurement data.

The WSC provides a simple method to describe the wind speed distribution with height [18], ignoring the influence of wind direction, atmospheric stability, surface roughness, and other factors. It is mainly used to describe the wind speed change in the vertical direction, while the wind speed gradient and eddy current in the horizontal direction cannot be effectively described. Although the PD model is more complex in calculation and more parameter dependent, it can provide more accurate wind speed extrapolation predictions.

The above research results prove that the WSC is crucial to the accuracy of wind resource extrapolation. However, the current research on the WSC usually does not consider atmospheric stability, and the improvement of wind resource assessment is rarely mentioned. In this paper, the WSC is indirectly calculated by using the relationship between the gradient Richardson number and the M-O length, and the wind speed extrapolation model considering atmospheric stability is established, which improves the accuracy of wind speed extrapolation and enhances the engineering practicability of the model.

This article mainly studies the influence of the wind speed extrapolation model considering atmospheric stability on wind resource assessment. The content of this article is as follows: In the Section 2, the power law model and M-O similarity theory are introduced, and the wind speed extrapolation model considering atmospheric stability is established. The Section 3 introduces the data source and the basic situation of the data. The Section 4 introduces the time-varying relationship between WSC and atmospheric stability. The Section 5 introduces the analysis of the results of three extrapolation methods.

The main contributions of this article are as follows:

1. The daily and monthly variation in the WSC at different height intervals is analyzed, and the time-varying relationship between WSC and atmospheric stability is analyzed.
2. By comparing three different wind speed extrapolation methods, the improvement of wind speed extrapolation accuracy considering atmospheric stability is further verified.
3. An indirect calculation method of the WSC based on the relationship between the gradient Richardson number and M-O length is proposed.

2. Background

2.1. The Power Law

The power-exponential wind profile is a simple and feasible solution in practical applications. This profile can be mathematically expressed as follows [19]:

$$V_2 = V_1(Z_2/Z_1)^\alpha \quad (1)$$

where V_1 and V_2 are the average wind speeds at heights Z_1 and Z_2 , respectively. α is the Hellman coefficient, also known as the wind shear coefficient (WSC), which is related to wind speed, roughness, atmospheric stability, and height difference [20]. Based on Equation (1), the Hellman coefficient α can be obtained from the following expression:

$$\alpha = \ln(V_2/V_1)/\ln(Z_2/Z_1) \quad (2)$$

When the observed V_2 is not available, α is typically set to 0.143 or 1/7. However, this assumption is accurate only under flat terrain in neutral atmospheric conditions [16].

2.2. Wind Shear Coefficient Model Considering Atmospheric Stability

Based on the M-O similarity theory [17] and a series of studies, Panofsky and Dutton [16] proposed an empirical expression for calculating the wind shear coefficient using atmospheric stability and roughness.

$$\alpha = \frac{\Phi_m(\bar{Z}/L)}{\ln(\bar{Z}/Z_0) - \Psi_m(\bar{Z}/L)} \quad (3)$$

where \bar{Z} (m) is the geometric mean height of observations at heights Z_1 and Z_2 .

$$\bar{Z} = (Z_1 Z_2)^{0.5} \quad (4)$$

For stability functions Φ_m and Ψ_m , approximations similar to those reported by Irwin [10] can be used.

In Equation (3), L represents the M-O length, which can be calculated directly. The required data for the direct calculation of L are typically not included in wind datasets. Therefore, this article utilizes the relationship between the gradient Richardson number R_i [21] and L to calculate L .

$$R_i = \frac{g}{T} \left[\frac{\Delta T}{\sqrt{Z_1 Z_2} \ln \frac{Z_2}{Z_1}} + \Gamma_d \right] \left[\frac{\sqrt{Z_1 Z_2} \ln \frac{Z_2}{Z_1}}{\Delta \bar{u}} \right]^2 \quad (5)$$

$$L = \frac{Z |1 - 0.19 R_i|}{R_i}, \quad R_i > 0 \quad (6)$$

$$L = \frac{Z}{R_i}, \quad R_i < 0 \quad (7)$$

where ΔT is the temperature difference between the heights Z_1 and Z_2 ; $\Delta \bar{u}$ denotes the wind speed difference between the two heights; T is the average absolute temperature of the gas layer; and Γ_d represents the dry adiabatic temperature reduction rate. Under various conditions, stability functions can be expressed as follows:

Stable conditions ($\bar{Z}/L > 0$):

$$\Phi_m(\bar{Z}/L) = 1 + 4.7(\bar{Z}/L) \quad (8)$$

$$\Psi_m(\bar{Z}/L) = -4.7(\bar{Z}/L) \quad (9)$$

Neutral conditions ($\bar{Z}/L \approx 0$):

$$\Phi_m(\bar{Z}/L) = 1 \quad (10)$$

$$\Psi_m(\bar{Z}/L) = 0 \quad (11)$$

Unstable conditions ($\bar{Z}/L < 0$):

$$\Phi_m(\bar{Z}/L) = [1 - Y(\bar{Z}/L)]^{-1/4} \quad (12)$$

$$\Psi_m(\bar{Z}/L) = -\ln \left[\frac{(\zeta_0^2 + 1)(\zeta_0 + 1)^2}{(\zeta^2 + 1)(\zeta + 1)^2} \right] - 2[\arctan(\zeta) - \arctan(\zeta_0)] \quad (13)$$

where

$$\zeta = [1 - \gamma(\bar{Z}/L)]^{1/4} \tag{14}$$

$$\zeta_0 = [1 - \gamma(Z_0/L)]^{1/4} \tag{15}$$

Z_0 is the roughness length, which can be obtained from the following expression [5,22]:

$$Z_0 = \exp\left[\frac{h_2^\alpha \ln(h_1) - h_1^\alpha \ln(h_2)}{h_2^\alpha - h_1^\alpha}\right] \tag{16}$$

3. Case Study

This article utilizes a dataset collected from a flat wind farm located in northern China. The wind farm has a 5 km radius, an average altitude of 10 m, and a 150 m high anemometer tower. The anemometer tower is surrounded by over 500 m of open farmland in all directions. Wind speed, wind direction, temperature, pressure, and air density were measured at heights of 2, 10, 50, 100, and 150 m with a time resolution of 15 min. The observation period began on 1 January 2014 and ended on 31 December 2014. This paper uses the three height intervals of 50–100, 50–150, and 100–150 m to evaluate the meteorological characteristics of the site, including the time-varying between the wind shear coefficient and the atmospheric stability. Meanwhile, the measured data of 100 and 150 m were utilized to compare the performance of various extrapolation methods.

4. Data Analysis

The analysis of the wind dataset reveals that the annual average wind speed and average wind power density are 4.34–6.22 m/s and 91.30–254.34 w/m², respectively. Accordingly, the annual average wind shear coefficient of the aforementioned height intervals can be calculated as follows: $\alpha_{50-100} = 0.234$, $\alpha_{50-150} = 0.226$, $\alpha_{100-150} = 0.231$.

Utilizing the gradient Richardson number method [21] incorporated with wind data, the Pasquale atmospheric stability grade is classified. The classification results are shown in Figure 1, indicating that the atmosphere is 57.27% unstable, 19.48% neutral, and 23.62% stable. Unstable (Class B) and relatively stable (Class E) classifications are not common (10.58% and 8.62%, respectively).

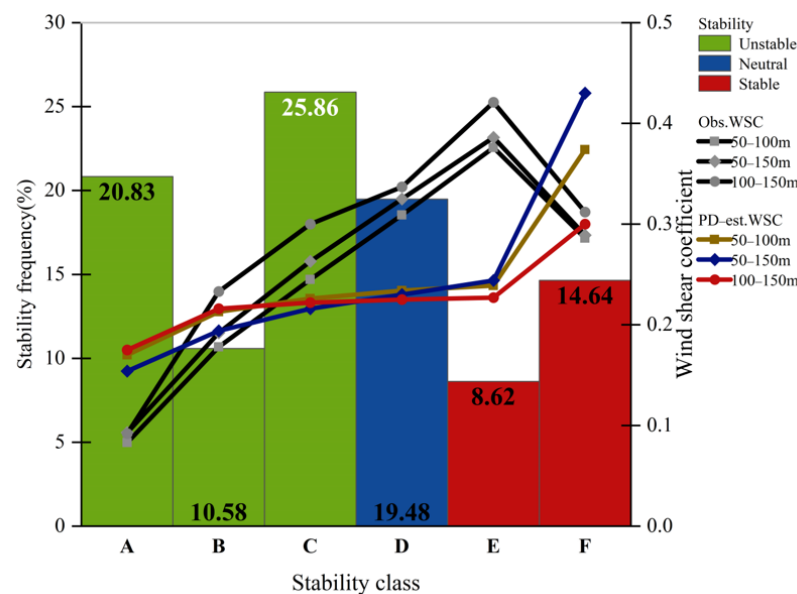


Figure 1. Variations in the annual mean WSC at a height of 50–150 m with atmospheric stability and the frequency of the Pasquale stability category.

Figure 1 indicates that the annual mean wind shear coefficient exhibits a positive correlation with the height interval and atmospheric stability. As the atmosphere changes from extremely unstable (Class A) to stable (Class F), the WSC increases to its highest value and reaches a relatively stable region (Class E). However, the WSC decreases slightly under stable conditions (Class F). This model is consistent with the findings reported by Gualtieri [12]. It is worth noting that the atmosphere condition is often unstable, and a constant predefined value for WSC (0.309–0.327), which corresponds to the neutral condition, is not consistent with the empirical coefficient.

Figure 1 also illustrates the variations in the annual mean wind shear coefficient obtained from the PD model (Equation (3)). It is observed that the WSC from Class B to Class D is underestimated. Moreover, the WSC of Class E is significantly underestimated, while the WSC of Classes A and F is overestimated. The results align with the findings reported by Irwin [10] and Zoumakis and Kelessis [23]. Overall, the annual average WSC predicted by the PD model is slightly lower than the annual average WSC of the observed data.

Figure 2 shows that at noon, the atmosphere is mostly unstable and the WSC is low. On the other hand, the atmosphere is mostly stable at night and the WSC is high. The diurnal variation of the WSC ranges from 0.270–0.309 around midnight to 0.073–0.112 at noon, with a difference of 176–270%. On the contrary, the difference in the annual variation of the WSC is not so obvious, exhibiting a difference of 30–60%, which is consistent with previous studies [7,12,24,25]. It is worth noting that the lowest WSC (0.175) occurs in July, coinciding with the mostly unstable atmosphere (81.15%). Conversely, stable conditions are infrequent (8.47%). This may be attributed to high surface heating during the day, which causes warm air to rise from the surface. When warm air rises, the pressure decreases and adiabatic expansion occurs. Meanwhile, the temperature of adiabatic expansion reduces to maintain thermodynamic equilibrium with the ambient temperature. If the temperature reduction is insufficient, hot air continues to rise and a large convective cluster is formed. Under this condition, large-scale turbulent vortices appear on the boundary layer. The boundary layer is also accompanied by vertical momentum exchange, resulting in relatively small changes in the average wind speed as the height increases. If warm air is excessively cooled during the ascending process, the vertical motion stops, which is called the stable layer. This surface phenomenon primarily occurs on cold nights. In this scenario, the surface friction is the determinant of the turbulence characteristics, and the wind speed changes significantly in the vertical direction. Therefore, daily variations in the WSC are closely related to the daily heating/cooling cycle of air above the ground, which is reflected by the atmospheric stability.

Figure 3 provides a two-dimensional diagram to compare the influence and interaction of the diurnal and annual changes in the WSC, concurrently.

Figure 3 illustrates notable changes in the WSC at both temporal and spatial scales. It also indicates that the WSC is high from 9:00 p.m. to 8:00 a.m. throughout the year, and the WSC at night is almost three times that during the day. The two-dimensional map of the WSC with time and month forms an elliptical 'solar shadow' caused by solar warming. This phenomenon is due to the high surface absorption of solar radiation during the day, which significantly warms the surface. A strong super-adiabatic temperature gradient forms between the surface and the atmosphere, and a positive (negative) net buoyancy appears for the upward (downward) vertical motion of the air mass, which accelerates the vertical motion and intensifies turbulent vortices. The higher momentum air in the upper layer mixes downward, and the wind speed in the lower layer is large and the vertical wind shear is small. This finding is consistent with reported observations in other locations [12,15,24,25], demonstrating that the phenomenon is also applicable elsewhere.

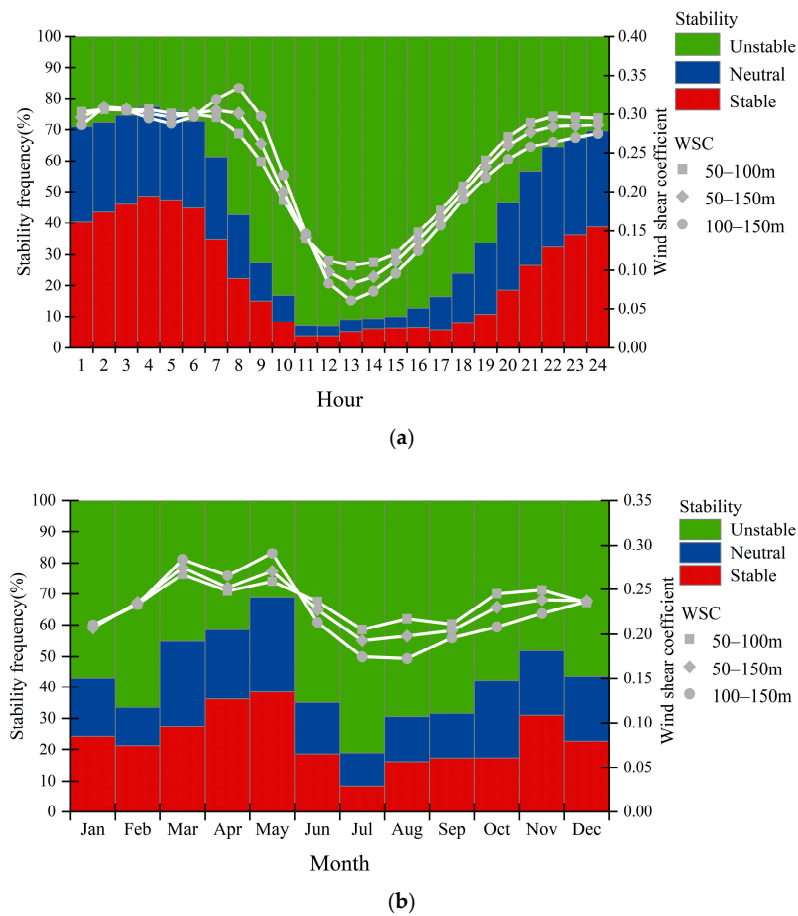


Figure 2. (a) Diurnal and annual variations in mean WSC under various atmospheric stabilities at a height of 50–150 m. (b) Annual mean WSC under various atmospheric stabilities at a height of 50–150 m.

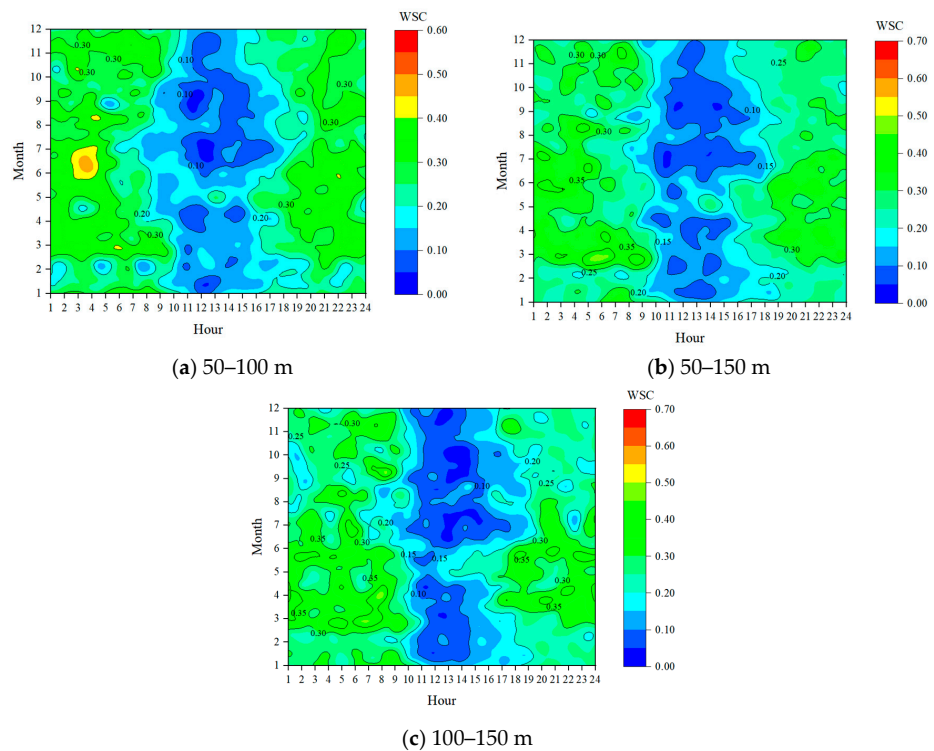


Figure 3. Two-dimensional variation of 10 min annual mean WSC at a height of 50–150 m.

5. Results and Discussion

5.1. Extrapolation Details

This article employs the PL model (Equation (1)) to extrapolate the wind speed (V_2) at the hub height ($Z_2 = 100, 150$ m) based on the wind speed (V_1) at the low-level height ($Z_1 = 50$ m). To this end, the following three approaches were followed: (1) utilizing the WSC at heights of 50–100 m and the wind speed at 50 m to extrapolate the wind speed at a height of 100 m; (2) employing the WSC at heights of 50–150 m and the wind speed at 50 m to extrapolate the wind speed at 150 m; (3) extrapolating the wind speed at 150 m based on the WSC at 100–150 m and the wind speed at 100 m. The WSC of the aforementioned approaches encompasses the following three options: (1) the annual average WSC; (2) the WSC incorporating stability changes; and (3) the calculation of the WSC using the PD model.

5.2. Wind Resource Extrapolation

5.2.1. Comparative Analysis of Extrapolation Methods

To evaluate the precision of models, the error between the extrapolated and observed wind speeds under different stability conditions is analyzed and normal bias (NB), normal root mean square error (NRMSE), correlation coefficient (R), and normal error (NE) are calculated. The annual average WSC, the WSC incorporating stability changes, and the PD model extrapolation evaluation between 50 and 150 m are analyzed as the main parameters, as shown in Tables 1–3.

Table 1. Extrapolated wind speed at 100 m under various atmospheric conditions based on data at 50 m.

	Stability Conditions			
	Unstable	Neutral	Stable	All
Observed				
N^1 (%)	20,021 (57.27)	6810 (19.48)	8131 (23.26)	34,962 (100)
V_o^2 (m/s)	5.6	7.37	4.39	5.67
Extrapolated from 50 m using $\alpha = 0.234$				
V_p^3 (m/s)	5.59	6.74	3.97	5.44
NB	0.002	0.089	0.102	0.041
NRMSE	0.056	0.100	0.145	0.088
R	0.993	0.996	0.979	0.987
Extrapolated from 50 m using stability-varying				
V_p (m/s)	5.42	7.17	4.25	5.49
NB	0.034	0.027	0.033	0.032
NRMSE	0.068	0.048	0.097	0.068
R	0.993	0.995	0.979	0.992
Extrapolated from 50 m using the PD model				
V_p (m/s)	5.69	7.05	4.41	5.65
NB	−0.017	0.048	−0.0002	0.002
NRMSE	0.058	0.062	0.088	0.065
R	0.989	0.995	0.978	0.989

¹ Number of measurements, ² mean measurements, ³ mean predictions.

Table 2. Extrapolated wind speed at a height of 150 m under various atmospheric conditions based on data at 50 m.

	Stability Conditions			
	Unstable	Neutral	Stable	All
Observed				
N^1 (%)	20,021 (57.27)	6810 (19.48)	8131 (23.26)	34,962 (100)
V_o^2 (m/s)	6.08	8.37	5.22	6.22

Table 2. Cont.

	Stability Conditions			
	Unstable	Neutral	Stable	All
Extrapolated from 50 m using $\alpha = 0.231$				
V_p^3 (m/s)	6.00	7.16	4.41	5.83
NB	0.013	0.156	0.168	0.065
NRMSE	0.098	0.171	0.238	0.143
R	0.979	0.985	0.949	0.966
Extrapolated from 50 m using stability-varying				
V_p (m/s)	5.80	8.11	4.99	5.95
NB	0.048	0.032	0.045	0.044
NRMSE	0.111	0.072	0.152	0.112
R	0.981	0.985	0.948	0.980
Extrapolated from 50 m using the PD model				
V_p (m/s)	5.88	7.94	5.65	6.17
NB	−0.010	0.075	−0.016	0.008
NRMSE	0.089	0.093	0.133	0.101
R	0.983	0.989	0.960	0.978

¹ Number of measurements, ² mean measurements, ³ mean predictions.

Table 3. Extrapolated wind speed at a height of 150 m under different atmospheric conditions based on data at 100 m.

	Stability Conditions			
	Unstable	Neutral	Stable	All
Observed				
N^1 (%)	20,021 (57.27)	6810 (19.48)	8131 (23.26)	34,962 (100)
V_o^2 (m/s)	6.15	7.68	5.71	6.22
Extrapolated from 100 m using $\alpha = 0.225$				
V_p^3 (m/s)	6.05	7.13	5.28	6.02
NB	0.016	0.074	0.080	0.033
NRMSE	0.049	0.086	0.109	0.067
R	0.996	0.995	0.991	0.994
Extrapolated from 100 m using stability-varying				
V_p (m/s)	6.13	7.69	5.94	6.25
NB	0.003	−0.002	−0.039	−0.004
NRMSE	0.045	0.038	0.073	0.050
R	0.995	0.998	0.991	0.997
Extrapolated from 100 m using the PD model				
V_p (m/s)	6.16	7.35	5.56	6.18
NB	−0.002	0.044	0.028	0.008
NRMSE	0.044	0.058	0.070	0.051
R	0.998	0.996	0.990	0.996

¹ Number of measurements, ² mean measurements, ³ mean predictions.

Table 1 indicates that the results have high R (0.987–0.992) and low NRMSE (0.065–0.088) indicating that extrapolation at heights of 50–100 m yields accurate results. However, it is found that using the annual average WSC and the WSC considering stability changes to extrapolate the wind speed at 100 m yields slightly underestimated results (NB = 4% when using the annual average WSC, and NB = 3% for the annual average WSC considering stability changes). On the other hand, the extrapolation error using the PD model is negligible (NB = 0.2%). Accordingly, it is inferred that the PD model is an appropriate approach for extrapolation. This is especially more pronounced under stable conditions (NB = 3%, NRMSE = 0.088).

Table 2 shows that extrapolation at heights of 50–150 m results in lower R (0.966–0.980) and higher NRMSE (0.101–0.143), reflecting lower calculation accuracy compared with extrapolation at 50–100 m. Similar to the previous part, the PD method exhibits different

behaviors under stable conditions. The results reveal that V150 was overestimated by 8% under stable conditions, slightly underestimated by 5% under neutral conditions, and achieved accurate results under unstable conditions (NB = 1%, NRMSE = 0.089). Compared with other approaches, the use of the WSC extrapolation considering stability changes significantly yields accurate results (NB = 3%, NRMSE = 0.07), especially under neutral conditions.

Table 3 demonstrates that the extrapolated values at 100–150 m achieved reasonable results for all 3 methods, and only the extrapolation using the annual average WSC is slightly underestimated (NB = 3.3%, NRMSE = 0.067). Moreover, in extrapolation using the WSC considering stability changes, significant improvements were achieved (NB = 0.4%, NRMSE = 0.050). This is especially more pronounced under neutral conditions, with negligible overestimation (NB = 0.2%). In general, for extrapolation at 100–150 m, the use of the WSC considering stability changes yields the best results, and the error is negligible under neutral conditions. Accordingly, the WSC extrapolation considering stability changes is recommended as the optimized approach for areas where the atmosphere is mostly neutral. By comparing with other studies [7,12,26,27], it is found that the higher the height of the extrapolated hub, the more obvious the advantages of using the PD model and the higher the accuracy of the prediction.

5.2.2. Time-Varying Analysis

In order to verify the accuracy and superiority of the PD model, the normal error (NE) of the wind speed extrapolated by the three methods was calculated, and two-dimensional maps of the time and annual changes of NE under different atmospheric stabilities were obtained. The results are presented in Figures 4–6.

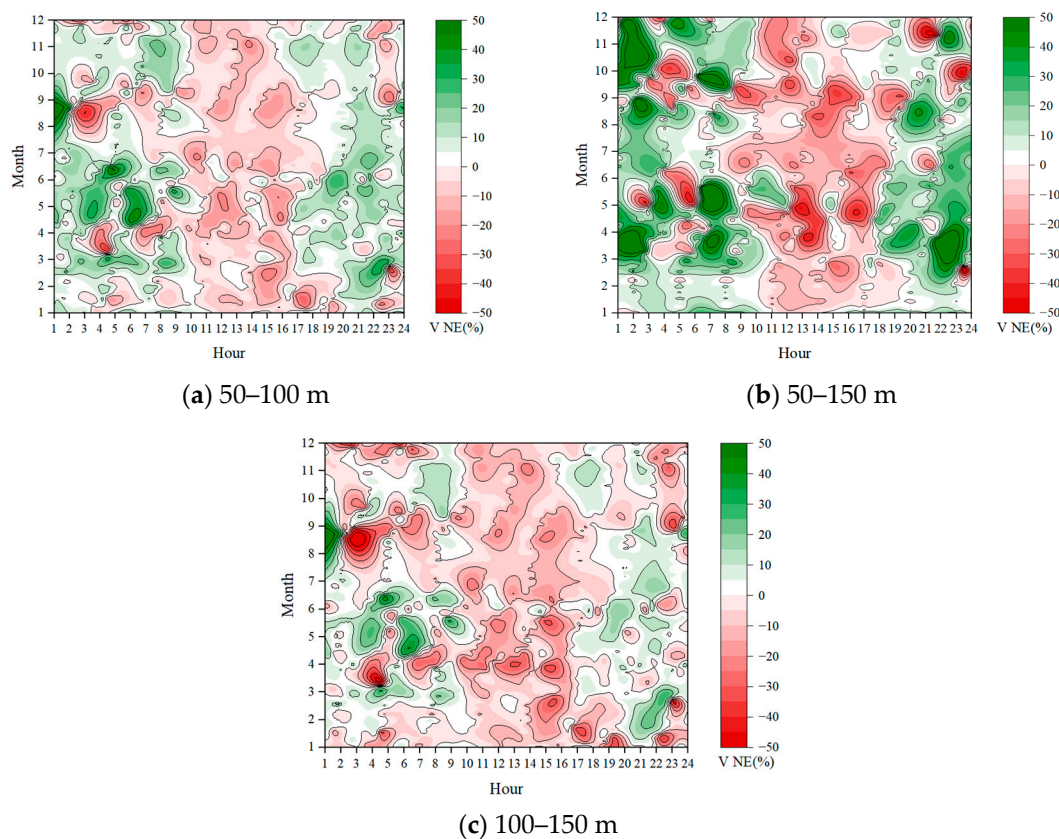


Figure 4. Two-dimensional variations in wind speed NE (%) obtained from annual average WSC.

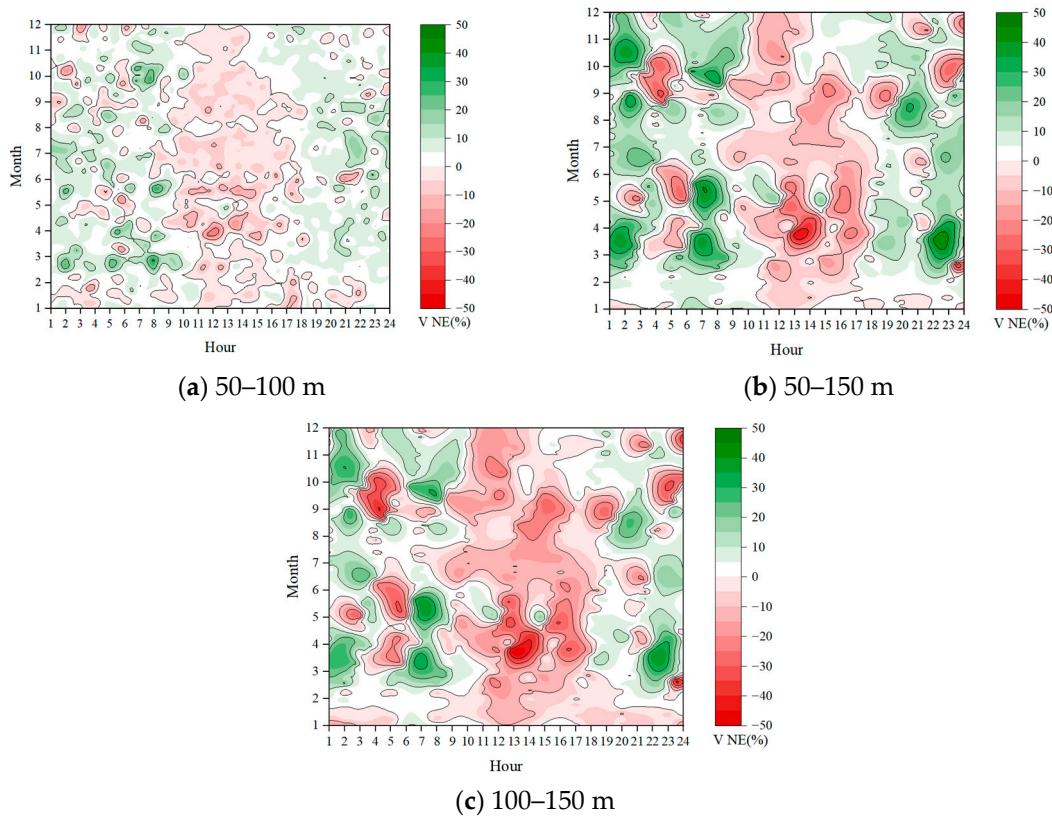


Figure 5. Two-dimensional variation in wind speed NE (%) obtained from WSC considering stability changes.

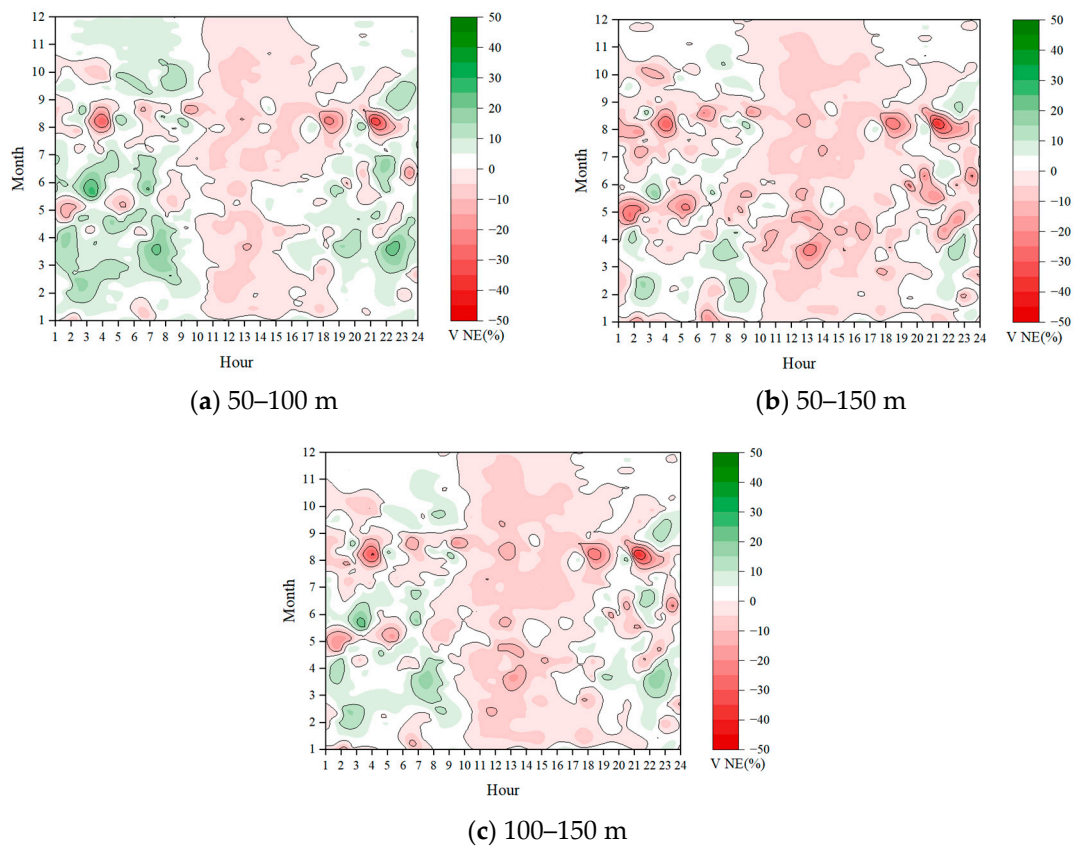


Figure 6. Two-dimensional variation in wind speed NE (%) obtained from the PD model.

Figure 4 reveals that the extrapolation of the annual average WSC leads to a significant overestimation during the day–night instability period, which almost coincides with the ‘solar shadow’ of the elliptical WSC in Figure 3. More specifically, unstable periods in April and October are overestimated by up to 45% when extrapolating between 50 and 150 m. The rest of the time, the extrapolation of wind speed is reasonable. In the stable period at night, it is recommended not to use the average WSC to extrapolate throughout the year but to use a WSC that takes into account changes in atmospheric stability. This is especially crucial in seasons with large temperature changes. When the atmosphere changes from an unstable to a stable boundary layer, the low-level jet stream occurs frequently, which greatly underestimates the wind speed of the hub height of large wind turbines. This finding aligns with the research conducted by Đurisić and Mikulović [26].

Figure 5 shows that if the WSC considering stability changes is used for extrapolation, the results improve significantly. When calculating the wind speed during unstable periods of day and night, especially in the extrapolation of 50–150 m, it leads to a certain overestimation and NE reaches 36%. The error of extrapolated wind speed in the rest of the time is small (NE < 20%), except for isolated peaks of the night hours in April and October where NE may exceed 30%.

Figure 6 shows two-dimensional variations in the extrapolated wind speed obtained from the PD model. It is observed that at 50–150 m and 100–150 m, the PD model outperforms the other schemes in terms of accuracy (NE < 25%). The superiority of the PD model is especially more pronounced during unstable periods of the day. It is also found that the PD model is more conservative in a more stable time at night. For instance, in the extrapolation of 50–150 m wind speed, the night-time extrapolation wind speed in May and August is overestimated and NE reaches 20%. However, the overestimation of night-time wind shear is a protection of the PD model against the potential threat of low-level jets to large wind turbines.

5.2.3. Weibull Distribution by Stability Condition

This paper also evaluates extrapolation methods by comparing the measured data with the Weibull distribution of the extrapolated wind speed. To emphasize the role of atmospheric stability, the Weibull distribution is classified according to the stability conditions, as shown in different atmospheric stability conditions in Figures 7–9.

At a height of 100 m, in both neutral (Figure 7b) and stable (Figure 7c) conditions, the Weibull distribution of wind speed, incorporating the influence of stability changes on WSC utilizing the PD model, aligns with the Weibull distribution of the measured wind speed. However, extrapolating using the WSC and considering stability-varying yields relatively less accurate results under unstable conditions. This is because the Weibull distribution is strongly affected by its shape parameters. Overall, employing the PD model for extrapolation yields accurate results with an error of less than 0.21. Additionally, the scale parameter exhibits the minimum error, with a value of 0.1 m/s.

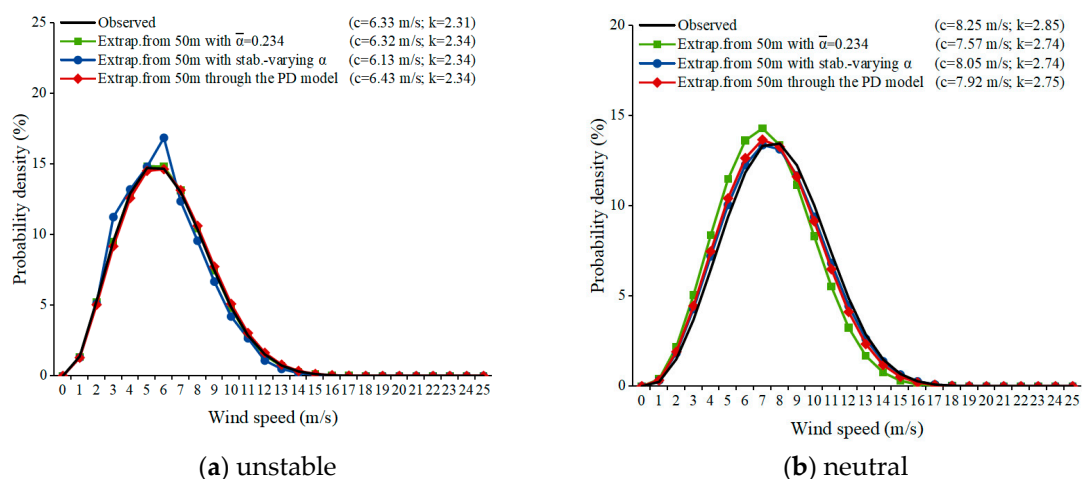


Figure 7. Cont.

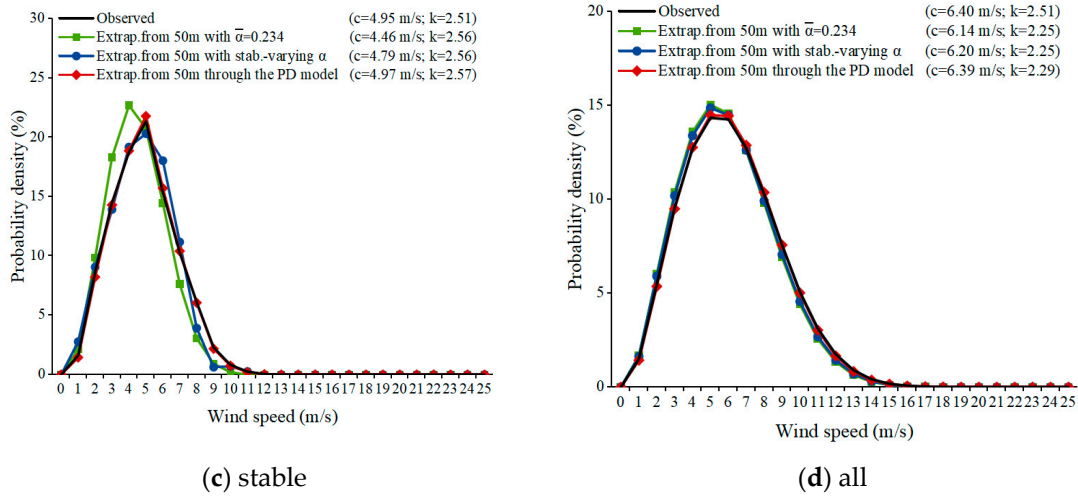


Figure 7. The comparison of the measured wind speed at 100 m with speed extrapolated using a Weibull distribution of 50–100 m.

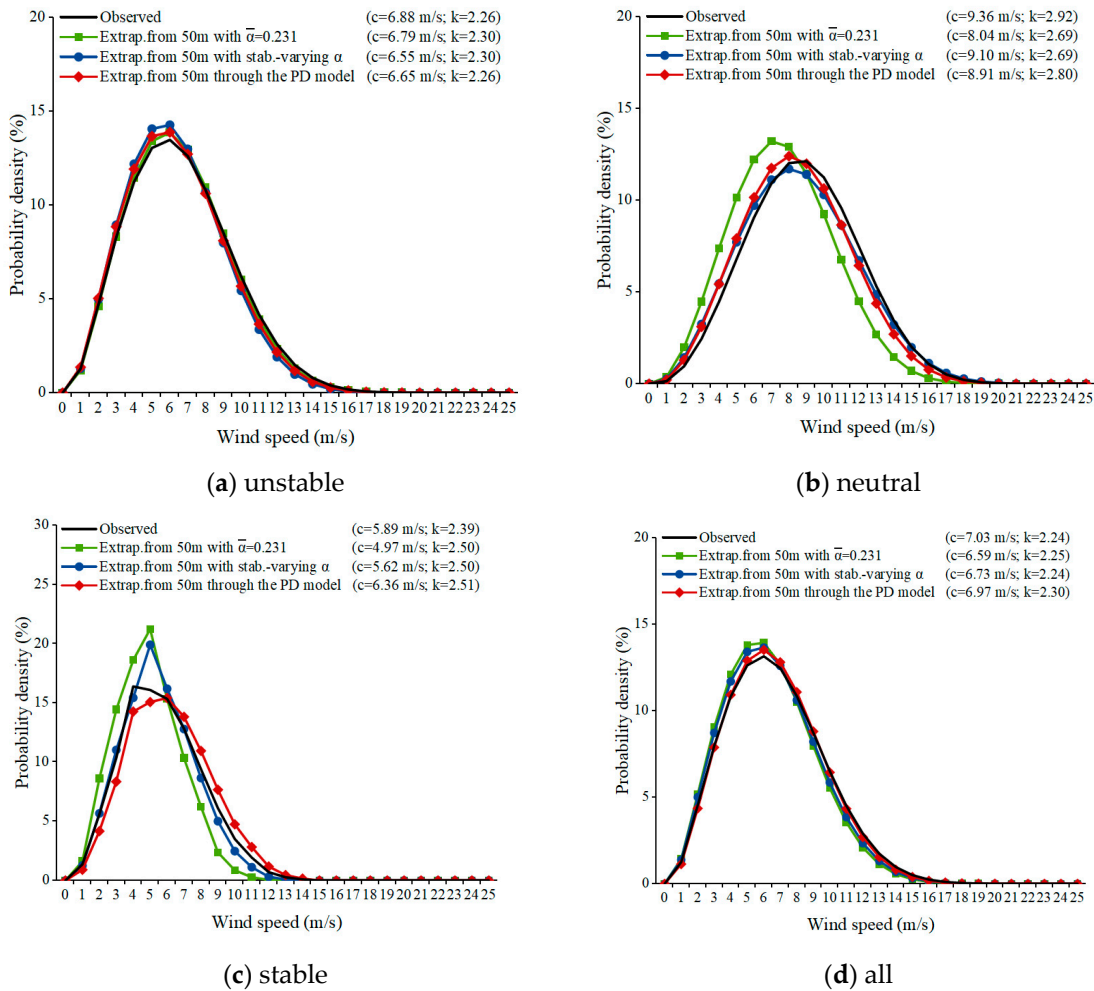


Figure 8. The comparison of the measured wind speed at 150 m with speed extrapolated using a Weibull distribution of 50–150.

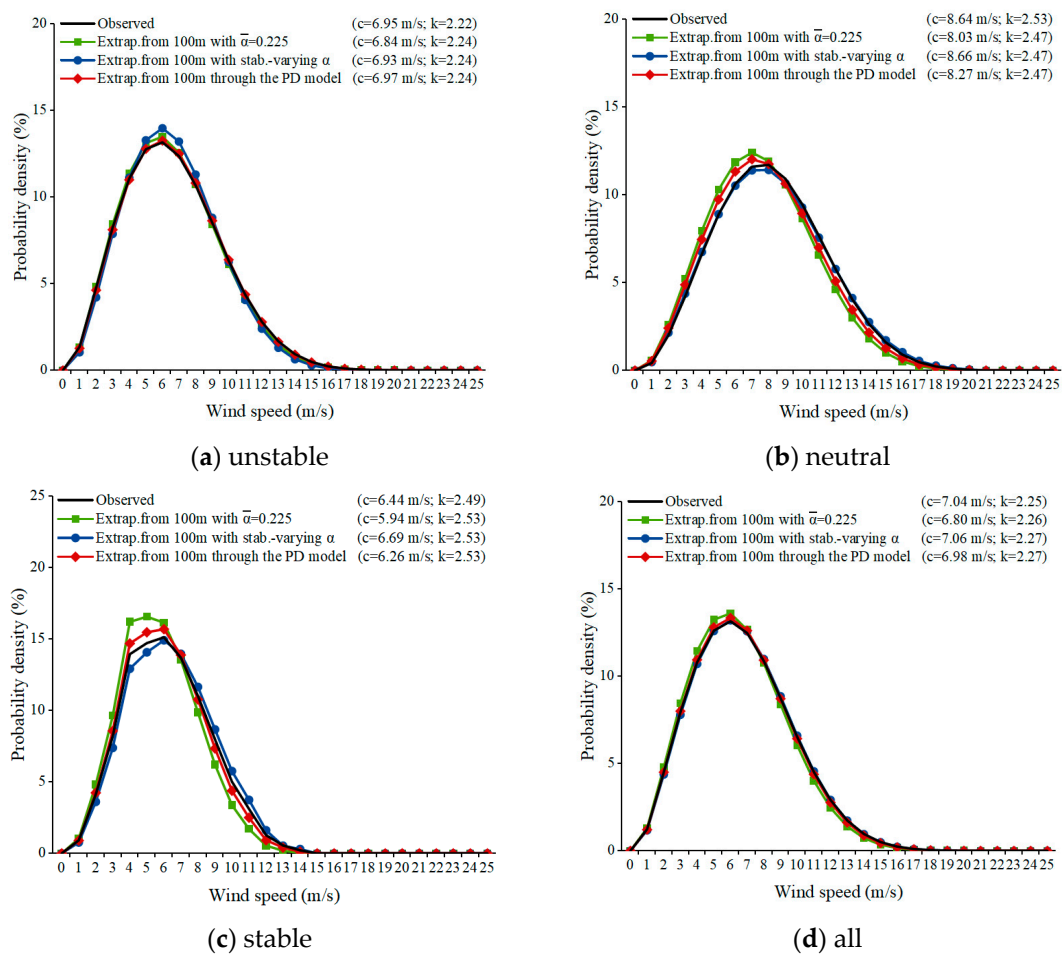


Figure 9. The comparison of extrapolated and measured wind speeds.

Figure 8c illustrates that under stable conditions, extrapolating wind speed between 50–150 m using the fitted WSC and the WSC considering stable changes results in significant inaccuracy, leading to a remarkable overestimation of the wind speed. However, the PD model still provides the best-fitting parameters. Under unstable conditions, the Weibull distribution extrapolated by the PD model exhibits similar accuracy to the observed wind speed. More specifically, their K parameters are consistent, and the difference is in the C parameter (0.23 m/s). This finding is consistent with the evaluation results of the extrapolation method in Table 2, indicating that the Weibull distribution can accurately fit the wind speed and reflect extrapolation errors.

Figure 9 shows that in the extrapolation between 100 and 150 m, the Weibull distribution is consistent with the results between 50 and 150 m, and the 3 methods exhibit reasonable accuracy. In addition, the parameters of the Weibull distribution of wind speed data at the same height are affected by the atmospheric conditions. Although the range of shape parameter K is small, the scale parameter C that determines the average wind speed distribution is affected by the atmospheric conditions. The more stable the atmosphere, the smaller the C value. This finding is consistent with the research carried out by Jingxin Jin et al. [27].

6. Conclusions

This paper focuses on the benefits of wind shear models considering atmospheric stability in the assessment of wind energy resources at hub heights. Recently, the PD model has been widely adopted as an accurate extrapolation model. In this regard, it is crucial to analyze the influence of affecting parameters such as friction temperature, friction velocity, and the von Karman coefficient on the performance of the PD model. In practical applications, anemometer towers are usually unobservable. The present study utilizes

the relationship between the M-O length and the gradient Richardson number to directly calculate the M-O length by using the wind-observed data. Based on the obtained results and performed analyses, the main conclusions can be summarized as follows:

1. The WSC is strongly affected by atmospheric stability. As the atmospheric condition changes from unstable to neutral and stable, the corresponding WSC increases from 0.174 to 0.309 and 0.319, respectively. Moreover, elliptical ‘solar shadow’ is caused by the increase in temperature.

2. For the 3 height intervals of 50–100, 50–150, and 100–150 m, the PD model extrapolation outperforms other methods in terms of accuracy. Compared with the annual average WSC extrapolation, the root mean square error (NRMSE) and the standard deviation (NB) of wind speed are reduced by 24–29% and 76–95%, respectively.

3. For 50–150 m, the extrapolation accuracy of the 3 methods is significantly lower than that of 50–100 m and 100–150 m. Therefore, it is of significant importance to select a reasonable height interval during extrapolation. The results demonstrate that the higher the extrapolated hub height, the more obvious the advantage of using the PD model.

4. When the atmosphere is mostly unstable or stable, the PD model outperforms other approaches in terms of extrapolation accuracy. However, the WSC extrapolation considering the stability changes is the recommended method under neutral conditions.

The proposed method is consistent with the observed wind speed data, but it still depends on the power law. The wind speed extrapolation from the lower layer to the hub height confronts high uncertainty. Therefore, it is essential to accurately assess the model uncertainty.

Although atmospheric stability analyses for wind energy applications have exhibited great advances, several challenges remain to be addressed. Among these challenges, it is possible to identify some areas that will become popular in the coming years:

- (1) Impact of climate change on short-term and long-term atmospheric stability.
- (2) Temporal and spatial variation of atmospheric stability in wind farms.

Author Contributions: Conceptualization, H.L. and G.C.; methodology, H.L. and G.C.; software, Z.H. and J.Z.; validation, H.L., G.C. and Z.H.; formal analysis, H.L., G.C. and Z.H.; investigation, H.L., G.C. and Z.H.; resources, H.L. and J.Z.; data curation, H.L.; writing—original draft preparation, H.L. and G.C.; writing—review and editing, H.L., G.C. and Z.H.; visualization, H.L., G.C. and Q.W.; supervision, Q.W.; project administration, Z.H. and Q.W.; funding acquisition, Z.H. All authors have read and agreed to the published version of the manuscript.

Funding: This research received no external funding.

Data Availability Statement: Due to the nature of this research, participants of this study did not agree for their data to be shared publicly, so supporting data is not available.

Conflicts of Interest: Author Jingang Zhang was employed by the company Suzhou THVOW Technology Co., Ltd. The remaining authors declare that the research was conducted in the absence of any commercial or financial relationships that could be construed as a potential conflict of interest. The Suzhou THVOW Technology Co., Ltd. had no role in the design of the study; in the collection, analyses, or interpretation of data; in the writing of the manuscript, or in the decision to publish the results.

References

1. REN21. *Renewables 2020: Global Status Report. Renewable Energy Policy Network for the 21st Century*; REN21: Paris, France, 2020; p. 302.
2. IEA. *Global Energy Review 2021*; IEA: Paris, France, 2021.
3. Li, J.; Yu, X. Analyses of the Extensible Blade in Improving Wind Energy Production at Sites with Low-Class Wind Resource. *Energies* **2017**, *10*, 1295. [[CrossRef](#)]
4. Wang, X.; Zeng, X.; Yang, X.; Li, J. Feasibility study of offshore wind turbines with hybrid monopile foundation based on centrifuge modeling. *Appl. Energy* **2018**, *209*, 127–139. [[CrossRef](#)]
5. Lackner, M.A.; Rogers, A.L.; Manwell, J.F.; McGowan, J.G. A new method for improved hub height mean wind speed estimates using short-term hub height data. *Renew. Energy* **2010**, *35*, 2340–2347. [[CrossRef](#)]
6. Crippa, P.; Alifa, M.; Bolster, D.; Genton, M.G.; Castruccio, S. A temporal model for vertical extrapolation of wind speed and wind energy assessment. *Appl. Energy* **2021**, *301*, 117378. [[CrossRef](#)]

7. Gualtieri, G.; Secci, S. Methods to extrapolate wind resource to the turbine hub height based on power law: A 1-h wind speed vs. Weibull distribution extrapolation comparison. *Renew. Energy* **2012**, *43*, 183–200. [[CrossRef](#)]
8. DeMarrais, G.A. Wind-speed profiles at brookhaven national laboratory. *J. Atmos. Sci.* **1959**, *16*, 181–190. [[CrossRef](#)]
9. Counihan, J. Adiabatic atmospheric boundary layers: A review and analysis of data from the period 1880–1972. *Atmos. Environ.* **1975**, *9*, 871–905. [[CrossRef](#)]
10. Irwin, J.S. A theoretical variation of the wind profile power-law exponent as a function of surface roughness and stability. *Atmos. Environ.* **1979**, *13*, 191–194. [[CrossRef](#)]
11. Firtin, E.; Güler, Ö.; Akdağ, S.A. Investigation of wind shear coefficients and their effect on electrical energy generation. *Appl. Energy* **2011**, *88*, 4097–4105. [[CrossRef](#)]
12. Gualtieri, G. Atmospheric stability varying wind shear coefficients to improve wind resource extrapolation: A temporal analysis. *Renew. Energy* **2016**, *87*, 376–390. [[CrossRef](#)]
13. Peterson, E.W.; Hennessey, J.P., Jr. On the use of power laws for estimates of wind power potential. *J. Appl. Meteorol. Climatol.* **1978**, *17*, 390–394. [[CrossRef](#)]
14. Wan, J.; Liu, J.; Ren, G.; Guo, Y.; Hao, W.; Yu, J.; Yu, D. A universal power-law model for wind speed uncertainty. *Clust. Comput.* **2019**, *22*, 10347–10359. [[CrossRef](#)]
15. Li, J.; Wang, X.; Xiong, Y. Use of spatio-temporal calibrated wind shear model to improve accuracy of wind resource assessment. *Appl. Energy* **2018**, *213*, 469–485. [[CrossRef](#)]
16. Panofsky, H.A.; Dutton, J.A. Atmospheric turbulence. In *Models and Methods for Engineering Applications*; Wiley: New York, NY, USA, 1984.
17. Monin, A.S.; Obukhov, A.M. Dimensionless characteristics of turbulence in the surface layer. *Akad. Nauk. SSSR Tr. Geofiz. Instituta* **1954**, *24*, 163–187.
18. Hua, Z.; Zhang, X.; Lu, K. Wind farm machine optimization analysis. *J. Northeast. Electr. Power Univ.* **2015**, *35*, 56–62. [[CrossRef](#)]
19. Hellman, G. Über die Bewegung der Luft in den untersten Schichten der Atmosphäre. *Meteorol. Z.* **1916**, *34*, 273–285.
20. Abbes, M.; Belhadj, J. Development of a methodology for wind energy estimation and wind park design. *J. Renew. Sustain. Energy* **2014**, *6*, 053103. [[CrossRef](#)]
21. Mohan, M.; Siddiqui, T.A. Analysis of various schemes for the estimation of estimation of atmospheric stability classification. *Atmos. Environ.* **1998**, *32*, 3775–3781. [[CrossRef](#)]
22. Bañuelose Ruedas, F.; Angelese Camacho, C.; Riose Marcuello, S. Analysis and validation of the methodology used in the extrapolation of wind speed data at different heights. *Renew. Sustain. Energy Rev.* **2010**, *14*, 2383–2391. [[CrossRef](#)]
23. Zoumakis, N.M.; Kelessis, A.G. Methodology for bulk approximation of the wind profile power-law exponent under stable stratification. *Bound.-Layer Meteorol.* **1991**, *55*, 199–203. [[CrossRef](#)]
24. Sisterson, D.L.; Hicks, B.B.; Coulter, R.L.; Wesely, M.L. Difficulties in using power laws for wind energy assessment. *Sol. Energy* **1983**, *31*, 201–204. [[CrossRef](#)]
25. Fox, N.I. A tall tower study of Missouri winds. *Renew. Energy* **2011**, *36*, 330–337. [[CrossRef](#)]
26. Đurišić, Ž.; Mikulović, J. A model for vertical wind speed data extrapolation for improving wind resource assessment using WASP. *Renew. Energy* **2012**, *41*, 407–411. [[CrossRef](#)]
27. Jin, J.; Li, Y.; Ye, L.; Xu, X.; Lu, J. Integration of atmospheric stability in wind resource assessment through multi-scale coupling method. *Appl. Energy* **2023**, *348*, 121402. [[CrossRef](#)]

Disclaimer/Publisher’s Note: The statements, opinions and data contained in all publications are solely those of the individual author(s) and contributor(s) and not of MDPI and/or the editor(s). MDPI and/or the editor(s) disclaim responsibility for any injury to people or property resulting from any ideas, methods, instructions or products referred to in the content.